



Influence of Blasting Vibrations Generated by Tunnel Construction on an Existing Road

Xianghui Deng¹ · Jingyuan Wang¹ · Rui Wang¹ · Qin Liu²

Received: 1 March 2020 / Revised: 5 July 2020 / Accepted: 9 July 2020 / Published online: 1 August 2020
© Iran University of Science and Technology 2020

Abstract

Tunnel excavations are commonly carried out using the drill and blast method, which may cause blast-induced damage to adjacent buildings. Peak particle velocity (PPV) is a widely used parameter for evaluating the damage of blasting vibration. However, accurately predicting PPV is difficult with traditional empirical predicting methods because their results are often different from actual conditions. In this study, attenuation formula of propagation velocity of elastic stress waves in elastomer is derived on the basis of stress wave theory. Moreover, the formula for predicting PPV is modified in the case of multihole and multistage blasting and then applied to Guanlinzi Tunnel, which downtraverses through National Highway 316. Results show that the modified formula obtains a small relative error between predicted and in situ monitoring PPVs and can properly reflect the propagation law of PPV under the condition of multihole and multistage blasting. This work has important application prospects and can provide a reference for similar excavation blasting and vibration control methods.

Keywords Shallow tunnel · Downtraversing · Existing road · Blasting vibration · Peak particle velocity · Field test

1 Introduction

The rapid development of traffic engineering has resulted in the remarkable growth of underground space utilization. Given the intensiveness of buildings, new tunnels will inevitably be constructed adjacent to existing buildings. New tunnels downtraverse existing roads in many cases because of the constraints of terrain and environmental and engineering geological conditions. Blasting vibration

during construction may damage the existing roads and endanger the safety of construction sites [1–3]. Therefore, evaluating the dynamic responses of existing roads subjected to blasting vibration and guaranteeing their safety during construction are necessary.

Many scholars have explored the influences of blasting vibration on existing structures through field experiments and numerical simulations. Yao et al. [4] numerically simulated the insufficient distance between the left and right lines in the excavation of Dong Jiashan Tunnel; the results of the study showed that construction blasting significantly influenced the constructed tunnel and the excavation of the upper and lower steps is conducive for the control of peak particle velocity (PPV). Through an overview of the blasting process and a description of various factors, Ainalis et al. [5] comprehensively reviewed and analyzed the approaches to model the blasting source and predict the propagation of ground vibrations accurately. Gui et al. [6] investigated the influence of rock–soil interface on blast wave propagation in the mixed rock–soil ground by numerically simulating blasting vibration velocity of key points along the horizontal and vertical

✉ Rui Wang
wangrui@xatu.edu.cn

Xianghui Deng
xianghuideng@xatu.edu.cn

Jingyuan Wang
15615557600@163.com

Qin Liu
chinlau@chd.edu.cn

¹ School of Civil and Architecture Engineering, Xi'an Technological University, Xi'an 710021, China

² School of Civil Engineering, Chang'an University, Xi'an 710048, China

directions; the results of the study indicated that rock–soil interfaces seriously influence the attenuation of rock blast wave. The development of test instruments has prompted many scholars to find solutions for these issues via field testing. Wang [7] used monitoring instruments to assess the impact of blasting vibrations; the results revealed that blasting vibration influences the lining structure of existing tunnels during the construction of the lower step and the effect on the lower step was greater than that on the upper step when the bench method was used to construct a new tunnel. Nateghi [8] analyzed the effects of different rock formations, detonators, and explosives; described ground motions induced by blasting near underground and surface concrete structures during the construction of Gotvand Dam; and selected PPV and frequency as the evaluation indices for analyzing the influence level of neighboring concrete structures in accordance with the United States Bureau of Mines. Many studies have used numerical simulation and field testing to obtain, analyze, and monitor data of blasting vibrations, velocity response, vibration attenuation, and acceleration response. Predicting PPV of key points in the theoretical formula according to the monitoring results is crucial, but studies have rarely focused on this issue. Therefore, establishing a theoretical method for predicting PPV is necessary.

2 Theoretical Analysis of Blasting Vibration Velocity

2.1 Problems in Predicting Blasting Vibration Velocity

In blasting engineering, blasting stress wave propagates in the medium and the blasting vibration velocity reflects the magnitude of the blasting stress wave energy [9, 10]. Therefore, the blasting vibration velocity is used as the evaluation index for assessing the impact on neighboring buildings [11–13]. In actual blasting engineering, predicting the vibration velocity of key points using theoretical methods is important but also complicated and difficult [14, 15]. Sadov's [16] and other empirical formulas are often used to predict PPV and obtain the blasting vibration velocity under different geological and construction conditions. The blasting vibration velocity can be predicted in some cases, and the maximum single-shot dose can be calculated reversely [17, 18]. Several scholars have proposed new prediction models considering the influencing factors of construction blasting [19, 20]. PPV (v) during cylindrical wave propagation is defined as follows:

$$v = \sqrt{\frac{r_b}{R} \frac{p_0}{\rho_0 C_L}}, \quad (1)$$

where r_b is the borehole radius, R is the distance from the blast source, p_0 is the pressure peak of borehole wall subjected to explosive blasting, ρ_0 is the rock density, and C_L is the propagation velocity of longitudinal wave in the elastic body.

Equation 1 shows that the blasting vibration velocity can be calculated in accordance with the borehole radius and the distance from the burst source. However, the results of this formula are often inconsistent with those of actual situations because it fails to reflect the terrain and geological and rock structural characteristics. Accordingly, (Eq. 1) must be modified in accordance with the actual situation. Lu et al. [21] combined the propagation characteristics of stress waves in actual rock mass and the spherical and long columnar drug wave theories to solve the problems mentioned above. Hence, the following vibration velocity formula is proposed for single-hole blasting:

$$\begin{cases} v = k v_0 (r_b/R)^\alpha \\ v_0 = p_0/\rho_0 C_0 \end{cases}, \quad (2)$$

where k and α are the coefficients related to the terrain and geology and the blasting vibration attenuation index, respectively, which are generally determined using field tests; v_0 is the PPV of borehole wall when r_b is equal to R ; and C_0 is the rock longitudinal wave velocity.

Wu et al. [22] proposed the following PPV formula considering multihole blasting on the basis of (Eq. 2):

$$v = k' k v_0 (r_b/R)^\alpha, \quad (3)$$

where k' is the correction coefficient under the same segment of multihole blasting related to the number of detonations in the same segment, position of calculation point, and hole connection. The effects of explosive type, charge structure, hole diameter, and rock mechanical parameters on the blasting vibration velocity can be determined according to (Eq. 3). However, (Eq. 3) has the following problems in predicting PPV during actual blasting engineering: (1) Using a single-hole radius r_b is clearly unreasonable because multihole and multistage detonation is often used in actual tunnel blasting and the selection of radius value should be in accordance with the situation of multihole and multistage detonation. (2) Determining the value of p_0 is difficult because charge coupling coefficients differ in actual blasting and the peak pressures on the borehole wall vary from the multisegment detonation approach used in blasting. (3) The correction factor k' value is difficult to determine in actual engineering. Although the multihole influential coefficient can be approximated to the

number of holes when the distance from the burst source is 400 times greater than the hole radius [23], this method has no theoretical basis and cannot confirm the parameters in practice.

2.2 Modification of the PPV Predicting Formula

Given that the values of r_b , p_0 , and k' are difficult to obtain, the existing and field test results will be combined to determine these parameters. The following ideas are presented in this study:

(1) Determining the equivalent radius r_e of multiple holes

r_b represents the single-hole radius, but the actual method used is the multihole and multistage blasting. Therefore, the equivalent borehole radius r_e is used to replace r_b . According to engineering experience and the results of related research, although many peripheral holes exist during blasting, the amount of noncoupling discontinuous charge is generally 1/3 to 1/2 of the auxiliary hole and the vibration impact is considerably smaller than that of auxiliary hole blasting. In addition, compared with the cutting hole, the positions of auxiliary holes are more dispersed and move toward the free surface when auxiliary holes are blasted. Therefore, the blasting vibration effect of auxiliary holes is still smaller than that of cutting holes despite its larger charge. Hence, the effect of typical oblique angles of cutting holes at 70° – 75° with a sine value of 0.94–0.97 can be ignored. In actual construction blasting, the different degrees of blasting vibration damage surrounding rock mass can be divided into smash district, crushing area, and elastic vibration zone. Multihole blasting is equated to single-hole blasting, and the equivalent blasting load is applied to the equivalent elastic boundary to simplify the calculation in this study. When the interaction of multihole blasting is ignored, the equivalent elastic boundary at the time of cutting hole blasting can be approximately equal to the envelope of the crushing zone at the blasting of each hole [24]. The equivalent radius of the borehole r_e is related to the radii of the smash r_1 and crushing r_2 zones (Fig. 1).

(2) Determining the equivalent peak pressure p_e .

The interaction of loads generated by multihole blasting forms the peak pressure of multihole blasting on the borehole wall. Therefore, the equivalent peak pressure p_e can be considered the product of the single-hole blasting peak pressure and the influence coefficient η . The stress wave propagating in the rock mass around the single borehole is attenuated in the form of an exponent. In this case, the equivalent peak pressure p_e on the borehole wall of the equivalent cutting hole can be calculated as follows:

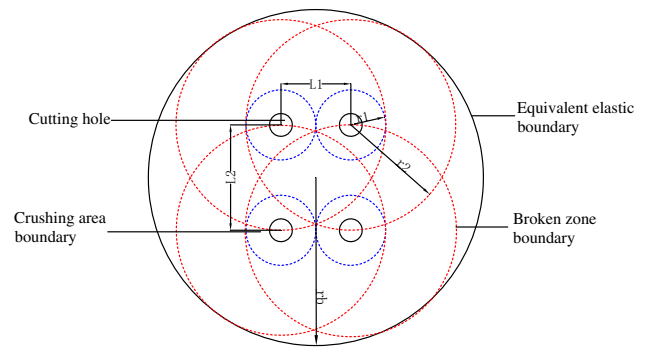


Fig. 1 Equivalent elastic boundary of cutting holes. a Top view b cross section view

$$p_e = \eta p_0 \left(\frac{r_b}{r_1} \right)^{2+\frac{\mu}{1-\mu}} \left(\frac{r_1}{r_2} \right)^{2-\frac{\mu}{1-\mu}} \tag{4}$$

where p_e is the equivalent peak pressure of multihole blasting on the borehole wall; p_0 is the peak pressure of single-hole blasting on the borehole wall; η is the effect index of load at the time of multihole initiation and related to the number and arrangement of holes; r_b is the borehole radius; r_1 and r_2 are the smash and crushing zone radii, respectively; and μ is the Poisson’s ratio of rock. When the columnar conventional explosive detonates, the radius of the smash zone is 3–5 times that of the charge and the radius of the crushing zone is 10–15 times that of the charge.

Uncoupled charge structures are often used in tunnel excavation blasting. According to Chapman–Jouguet’s theory of detonation wave of condensed state explosives, the peak pressure of single-hole wall under the condition of uncoupling charge is calculated as follows:

$$p_0 = \frac{\rho_e D^2}{2(\gamma + 1)} \left(\frac{d_c}{d_b} \right)^6 \tag{5}$$

where ρ_e is the explosive density, D is the explosive detonation speed, γ is the isentropic index with a common value of 3.0, d_c is the charge diameter, and d_b is the borehole diameter.

In the case of multihole initiation, the load influence coefficient is determined as follows:

$$\eta = \frac{n\pi r_2^2}{\pi r_e^2} = n \cdot \left(\frac{r_2}{r_e} \right)^2 \tag{6}$$

where n is the number of cutting holes and r_e is the equivalent elastic boundary radius of cutting holes.

(3) Modified formula in the case of multihole and multistage blasting.

According to the principle of equivalence, the entire inelastic zone formed by multihole blasting can be equivalent to a single-blast source. Thus, the correction coefficient k' is approximately equal to 1.0. Therefore, the theoretical formula for predicting PPV in the case of multihole and multistage blasting can be expressed as.

$$\begin{cases} v = kv_e(r_e/R)^{\alpha} \\ v_e = P_e/\rho_0 C_0 \\ P_e = \eta p_0(r_b/r_1)^{2+(\mu/1-\mu)}(r_1/r_2)^{2-(\mu/1-\mu)} \\ p_0 = [\rho_e D^2/2(\gamma + 1)](d_c/d_b)^6 \\ \eta = n \cdot (r_2/r_e)^2 \end{cases} \quad (7)$$

The explosive types, charge structure, hole diameter, and mechanical parameters of rock considered in (Eq. 7) have clear physical meanings.

2.3 Comparison of the Modified Model with Other Models

The results of Sadoy's formula are inconsistent with those of actual situations because the formula fails to reflect the terrain and geological and rock structural characteristics. Lu [21] subsequently proposed a modified formula that considers the drawbacks of Sadoy's formula. However, this modified formula is difficult to apply in actual engineering because the values of parameters r_b , p_0 , and k' are difficult to determine in multihole and multistage blasting although the effects of explosive type, charge structure, hole diameter, and mechanical parameters of rock on PPV can be determined. In this study, a theoretical formula considering the explosive types, charge structure, hole diameter, and mechanical parameters of rock is proposed for predicting PPV in the case of multihole and multistage blasting. The parameters are determined according to the results of existing studies and the field blasting test.

3 Brief Description of the Project

The Guanlinzi Tunnel consisting of six two-way lanes is part of the Baoji to Hanzhong Expressway in China. The lengths of the left and right lines are 420 and 509 m, respectively. The net height and width of the construction limit are 5.0 and 14 m, respectively. The Guanlinzi Tunnel belongs to a superlarge cross section tunnel with an excavation area of 158.8 m². A mountain and a river can be found on the respective left and right sides of National Highway 316 with the new tunnel undercrossing the highway. The color and structure of the surrounding rock

made of strong weathered gneiss with developing joints and fissures are light greyish brown and crystal, respectively.

3.1 Relative Position of the New Tunnel and National Highway 316

The Guanlinzi Tunnel is on the right bank of Baohe River. The distance between the left and right exits of the tunnel is 34 m. The left line of the tunnel obliquely crosses the National Highway 316 at 40° in the section between ZK159 + 719.9 and ZK159 + 750.18. The minimum depth of covering soil is only 6.07 m at the ZK159 + 733 section. The right line of the tunnel obliquely crosses National Highway 316 at 45° in the section between YK159 + 781.09 and YK159 + 818.25. The minimum depth of covering soil is only 4.05 m at the YK159 + 801 section. The location relationship between the new tunnel and the existing road is shown in Figs. 2 and 3. The results show that the terrain and geological conditions of the project are complex. National Highway 316 is an important channel that connects Hanzhong to Baoji. Serious traffic flows in this channel are usually caused by large trucks. Therefore, ensuring the safety of the new tunnels and National Highway 316 is important but difficult when tunnel construction blasting is adopted.

3.2 Construction Method and Support Parameters of the Tunnel

Given that the surrounding rock of the downtraversing section made of strong weathered gneiss is classified under grade V, the double $\Phi 159 \times 10$ mm presupport pipe shed is used to reinforce the tunnel. The excavation of the tunnel portal section is carried out using the cross-diaphragm (CRD) method. (Construction procedures are shown in Fig. 4.) The preliminary support structure is designed as follows: The entire face of C25 shotcrete with a thickness of 28 cm is sprayed. A 20 cm \times 20 cm double $\Phi 8$ steel mesh hangs on the arch wall. A I22b-type steel frame is set in the entire section with a spacing of 50 cm between the pins. $\Phi 22$ grouted bolts have a length of 4.0 m. A plum-shaped arrangement of 100 cm \times 100 cm is constructed at the sidewall. C30 reinforced concrete with cross-sectional thickness of 60 cm is used in the secondary lining structure and strengthened with a grid steel frame, which consists of four main $\Phi 22$ reinforcements and $\Phi 12$ stirrups. By placing intervals between the steel frames, the stirrup and steel grid spacings are set to 20 and 50 cm, respectively. Temporary support and inverted arch are protected by the 22-cm-thick shotcrete and anchorage. Eleven advanced small pipes with a spacing of 40 cm between them and outer angle of 12°

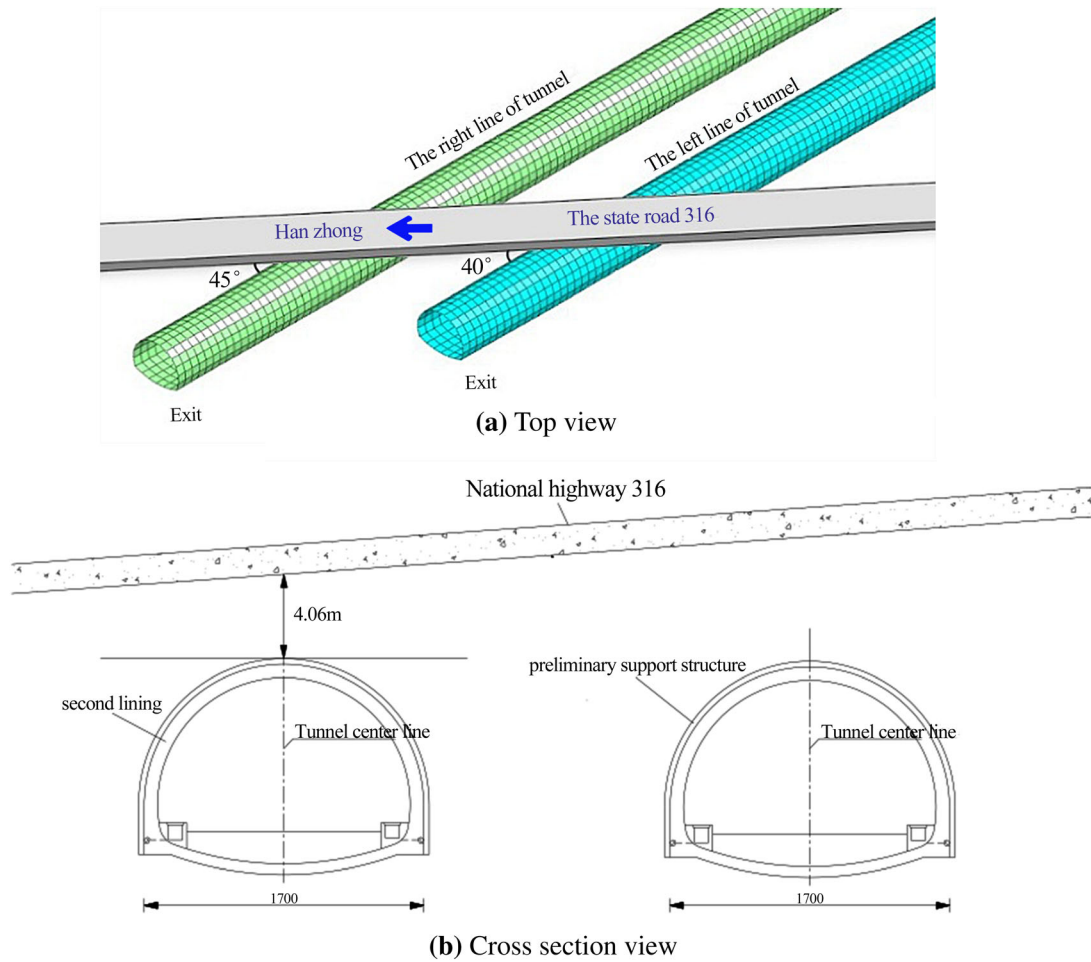


Fig. 2 Relationship between the new tunnel and the existing road



Fig. 3 Actual situation of the new tunnel under National Highway 316

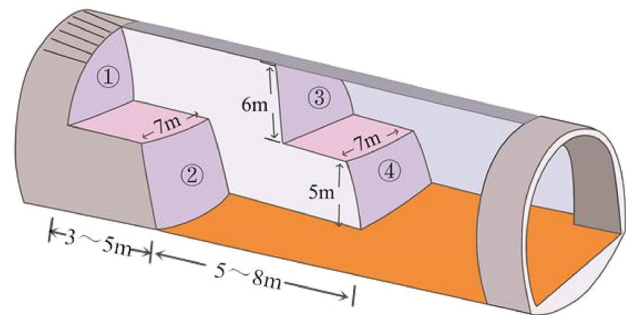


Fig. 4 Excavation diagram of the CRD method

are used in the temporary supports. The early-strength grouted bolts are set with a spacing of 1 m along the temporary supports.

4 Results and Discussion

4.1 Blasting Scheme

Tunnel footage is 1.0 m in the CRD construction method. Smooth blasting is adopted for excavation, and the cutting holes have a wedge-shaped groove structure with a drilling depth of 1.2 m. The upper left and right parts have 37 and 24 peripheral holes, respectively, with a distance of 50 cm and depth of 1.0 m. The explosive charges of the upper left and right parts are 27.8 and 26.4 kg, respectively. Seven-segment delay detonators are used in blasting. The blasting scheme is shown in Fig. 5, and the blasting parameters are listed in Tables 1 and 2.

4.2 Field Monitoring Scheme of Blasting Vibration

Given that the minimum distances between the left and right lines of the new tunnel and National Highway 316 are 6.07 and 4.05 m, respectively, the structural safety of National Highway 316 is seriously threatened by tunnel construction blasting. According to the unfavorable principle, the monitoring section of blasting vibration must be set in the most unfavorable position of the existing road nearest to the blasting source. Five monitoring points are distributed in the scheme of the monitoring section. The corresponding road point directly above the tunnel vault is considered the base point (denoted point 0), while the monitoring points shown in Fig. 6 are distributed on the left and right sides of the base point.

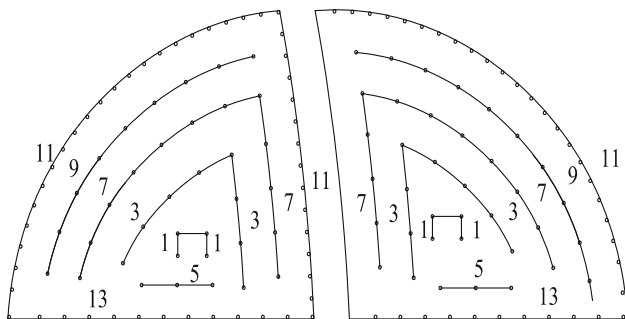


Fig. 5 Design of tunnel blasting scheme

4.3 Arrangement and Installation of Monitoring Instruments

A TC-4850 blasting vibration recorder is used in the field test. The observation system of blasting vibration effect is composed of a TCS-B3-type three-way vibration velocity sensor, low-noise shielding cable, and computer. The installation process of instruments is presented as follows: (1) Use a brush to clean the location of the desired distribution point, which is conducive to the close connection of gypsum and the ground. (2) Prepare a viscous solution made of gypsum powder and water and then apply it evenly to the cleaned surface. Ensure that the horizontal direction is facing backward (blasting is generally conducted in the direction of sensor X pointing to the blast center), press the three vector sensors with the palm, and drive the sensor to the left and right directions during the force process to prevent uneven adhesion and formation of air bubbles between the sensor and the plaster as well as improve the rigid connection between the sensor and the inspected surface. (3) Add gypsum powder around the sensor to absorb excess water and accelerate the setting rate of gypsum. According to several tests, the maximum vibration velocity of tunnel blasting is 1.5 cm/s. The trigger level value is set to 0.3 cm/s to collect a valid signal and prevent the nearby vibration interference signal from triggering the instrument. According to engineering experience and the delay detonator segment, each blasting time should be approximately 1.0 s under normal circumstances. Therefore, the burst vibrator cycle time is set to 2 s with a delay of – 100 ms in this test. Confirm the location of the tunnel vault and the pavement base point as the reference point prior to construction blasting. The monitoring points in this test are set every 5.0 m on both sides of the reference point with five monitoring points in each section. Gypsum slurry with a water/cement ratio of 1:3.5 is prepared. The sensor is fixed on the monitoring point. The X-axis of the sensor is parallel to the blasting surface, the Y-axis is pointing to the blasting plane, and the Z-axis is arranged perpendicular to the horizontal plane. Activate the blasting vibration recorder and initiate data collection. The equipment layout is illustrated in Fig. 7.

4.4 Analysis of Field Test Results

The blasting tests are carried out in the cross sections of the new tunnels ZK159 + 727 and ZK159 + 733. The segmented delay method is adopted for the blasting scheme, and the blasting vibrator parameters are set before the test to avoid overlapping of the seismic waveforms generated by each burst. The test results are presented in Tables 3 and 4. The maximum vibration velocities in the upper left and

Table 1 Blasting parameters of the upper left part by the CRD method

Excavation site	Serial number	Name of the borehole	Borehole depth (m)	Detonator level (segment)	Number of holes (one)	Single hole charge (kg)	Total charge (kg)
Upper left part	1	Cutting hole	1.2	1	4	0.8	3.2
	2	Auxiliary hole	1.0	3	8	0.4	3.2
	3	Auxiliary hole	1.0	5	3	0.4	1.2
	4	Auxiliary hole	1.0	7	12	0.4	4.8
	5	Auxiliary hole	1.0	9	9	0.4	3.6
	6	Peripheral hole	1.0	11	37	0.2	7.4
	7	Bottom plate hole	1.0	13	11	0.4	4.4
Subtotal					71		27.8

Table 2 Blasting parameters of the upper right part by the CRD method

Excavation site	Serial number	Name of the borehole	Borehole depth (m)	Detonator level (segment)	Number of holes (one)	Single hole charge (kg)	Total charge (kg)
Upper right part	1	Cutting hole	1.2	1	4	0.8	3.2
	2	Auxiliary hole	1.0	3	8	0.4	3.2
	3	Auxiliary hole	1.0	5	3	0.4	1.2
	4	Auxiliary hole	1.0	7	12	0.4	4.8
	5	Auxiliary hole	1.0	9	10	0.4	4.0
	6	Peripheral hole	1.0	11	24	0.2	6.0
	7	Bottom plate hole	1.0	13	10	0.4	4.0
Subtotal					71		26.4

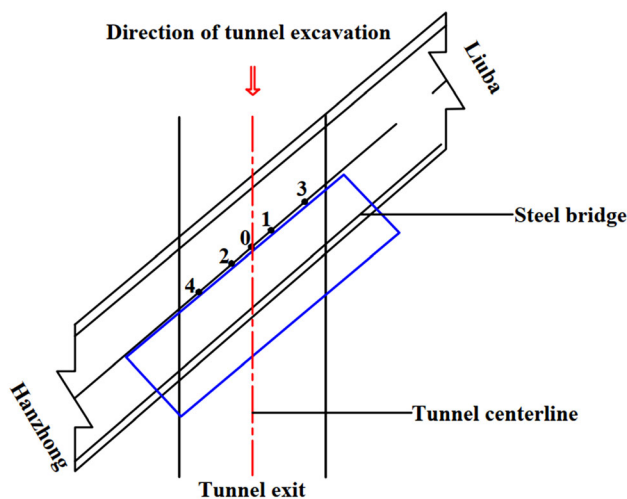


Fig. 6 Distribution of blasting vibration monitoring points

right parts of the excavation section are shown in Figs. 8 and 9, respectively.

PPV is shown in the monitoring results of the cut blasting. Table 3 and Fig. 8 show that the maximum and minimum vibration velocities of blasting in the upper left

part of ZK159 + 727 cross section occurring at key points 1 and 4 are 0.55 and 0.32 cm/s, respectively. The maximum and minimum vibration velocities of blasting in the upper right part occurring at key points 2 and 4 are 0.55 and 0.30 cm/s, respectively. As shown in Table 4 and Fig. 9, the maximum and minimum vibration velocities of blasting in the upper left part occurring at key points 1 and 4 of ZK159 + 733 cross section are 1.32 and 0.36 cm/s, respectively. The maximum and minimum vibration velocities of blasting in the upper right part occurring at key points 2 and 3 are 1.24 and 0.55 cm/s, respectively. According to the velocity distribution results, the small PPV values and the spatial distribution of PPVs characterized by a “large middle and two small ends” are consistent with the actual situation.

4.5 Determining the Relevant Parameters of the Formula

Regression analysis is applied on the basis of the blasting test results to determine the relevant parameters of (Eq. 7), which is proposed by the authors. The charging parameters are determined in accordance with the actual situation and related specifications. Explosive density ρ_e , explosive

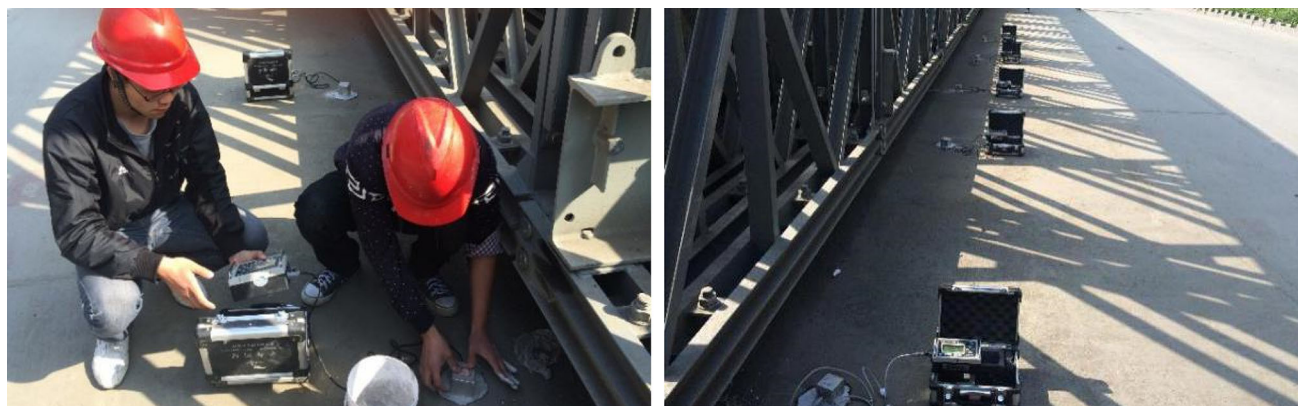


Fig. 7 Monitoring instrument layout

Table 3 Vibration velocities and related parameters for the key points of ZK159 + 727 section

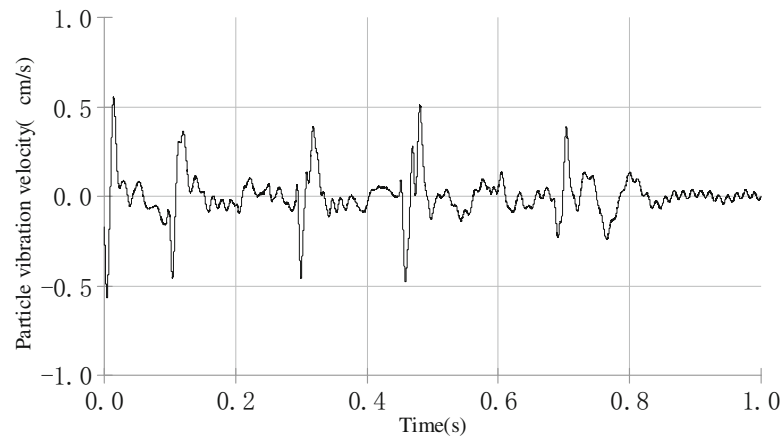
Blasting parts	Measuring point number	Number of segments of maximum vibration velocity	Maximum velocity direction	One-way maximum particle velocity (cm/s)	Blasting center distance R (m)
Upper left part	3	One segment	Z	0.40	15.89
	1	One segment	Z	0.55	15.21
	0	One segment	Z	0.52	15.65
	2	One segment	Z	0.41	17.28
	4	One segment	Z	0.32	20.89
Upper right part	3	One segment	Z	0.36	20.21
	1	One segment	Z	0.43	17.02
	0	One segment	Z	0.50	15.87
	2	One segment	Z	0.55	15.45
	4	One segment	Z	0.30	17.01

Table 4 Vibration velocities and related parameters for the key points of ZK159 + 733 section

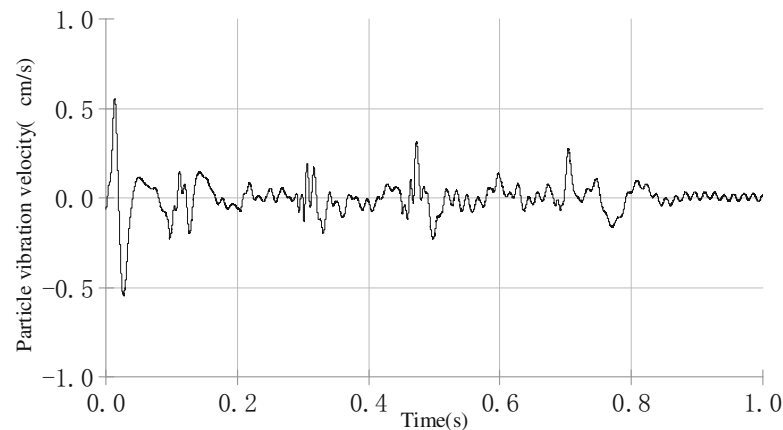
Blasting parts	Measuring point number	Number of segments of maximum vibration velocity	Maximum velocity direction	One-way maximum particle velocity (cm/s)	Blasting center distance R (m)
Upper left part	3	One segment	Z	0.89	12.15
	1	One segment	Z	1.32	11.37
	0	One segment	Z	0.71	11.87
	2	One segment	Z	0.52	13.49
	4	One segment	Z	0.36	17.00
Upper right part	3	One segment	Z	0.55	16.31
	1	One segment	Z	0.85	13.20
	0	One segment	Z	1.17	11.91
	2	One segment	Z	1.24	11.68
	4	One segment	Z	0.73	13.20

detonation speed D , charge diameter d_c , and borehole diameter d_b are determined in accordance with the blasting manual. The density of grade V surrounding rock ρ_0 is set to 2.0 g/cm^3 on the basis of the Highway Tunnel Design Code (JTG D70-2014) in China. Similarly, the longitudinal

wave velocity is chosen in accordance with the norms of Rock Bolt and Shotcrete Support Engineering Technical Specifications (GB50086-2015) in China. The parameters are listed in Table 5.



(a) Measured value of blasting vibration velocity of the key point 1 for the upper left part excavation



(b) Measured value of blasting vibration velocity of the key point 2 for the upper right part excavation

Fig. 8 Maximum vibration velocities of the key point of ZK159 + 727 section (Z direction)

The relevant parameters k and α of (Eq. 7) can be obtained using regression analysis. The regression fitting curve and related parameters are illustrated in Fig. 10. According to the results of 20 test points in the field, the coefficient k related to the terrain and geology and the blasting vibration attenuation index α are 31.58 and 2.261, respectively. Therefore, the fitting curve of PPV is obtained as follows:

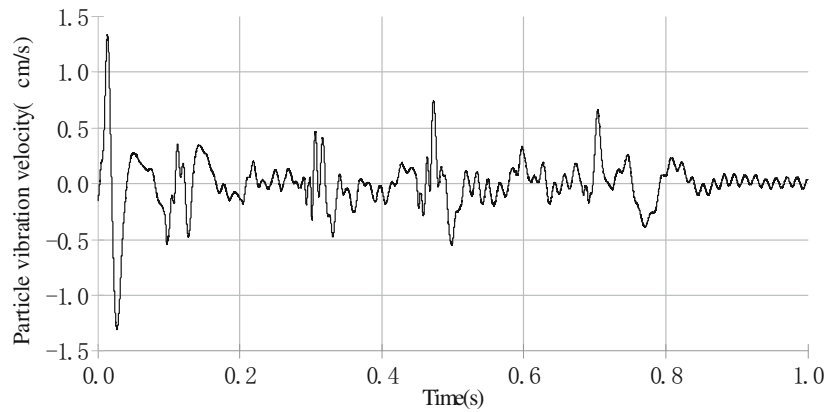
$$v = 493.24 \times (0.818/R)^{2.261} \quad (8)$$

The correlation analysis of test results shows that the correlation coefficient R^2 value of 0.818 of the fitting curve accurately reflects the vibration velocity distribution of road surface.

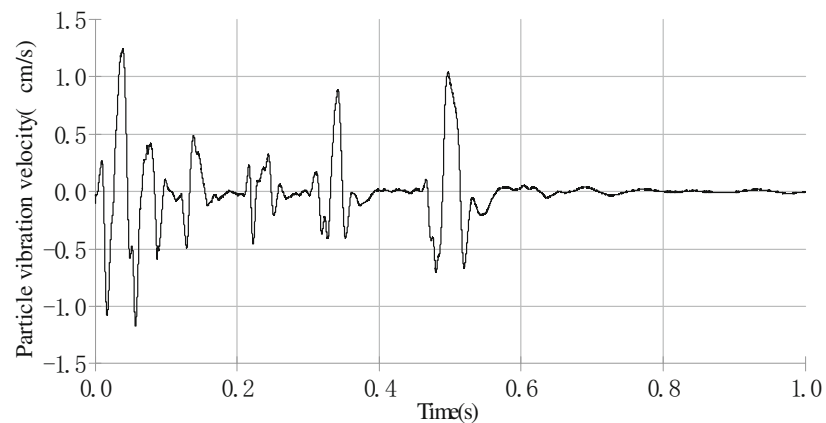
4.6 Comparative Analysis of Measured and Predicted Values

The blasting vibration test is performed in the upper left and right parts of the YK159 + 801 cross section of the new tunnel to verify the reliability of the formula. The results are presented in Table 6 and Fig. 11. Table 6 shows that PPV is predicted using both the proposed and Sadov's formulas. The predicted results and relative errors with measured values are listed in Table 6.

The monitoring results demonstrate that the maximum PPV appears in the blasting of cutting holes. When Sadov's formula is adopted to predict PPV, the maximum vibration velocities of blasting in the upper left and right parts are 8.04 and 8.41 cm/s, respectively. The error range is 197.5%–408.26%. The PPV values predicted using Sadov's formula have larger errors than those of the



(a) Measured value of blasting vibration velocity of the key point 1 for the upper left part excavation



(b) Measured value of blasting vibration velocity of the key point 2 for the upper right part excavation

Fig. 9 Maximum vibration velocities of the key point of ZK159 + 733 section (Z direction)

Table 5 Blasting parameters

Relative parameters	Borehole diameter d_b (mm)	Charge diameter d_c (mm)	Poisson's ratio μ	Rock density ρ_0 (g/cm^3)	Longitudinal wave velocity C_0 (m/s)	Explosive density ρ_e (g/cm^3)	Charge velocity D (m/s)
Values	42	32	0.35	2.0	2000	1.0	3500

measured results. Therefore, Sadov's formula is difficult to apply to this type of complex engineering. The maximum and minimum PPV values of blasting in the upper left part occurring at key points 1 and 4 are 2.19 and 0.61 cm/s, respectively, when the modified formula is adopted in this study. The maximum PPV occurring at key point 1 and minimum vibration velocity occurring at key point 4 are 2.35 and 0.56 cm/s, respectively, in the measured test. The maximum and minimum predicted PPV values of blasting in the upper right part of the tunnel occurring at key points

2 and 3 using the modified formula are 2.13 and 0.61 cm/s, respectively. In the measured test, the maximum and minimum vibration velocities occurring at key points 2 and 3 are 2.09 and 0.52 cm/s, respectively. The velocity distribution of the test results is similar to those of ZK159 + 733 and ZK159 + 727. The distribution law of PPVs demonstrates that the section far from the blast source has a small vibration velocity in different sections and the vibration velocity gradually decreases with increasing distance in the same section. The distribution

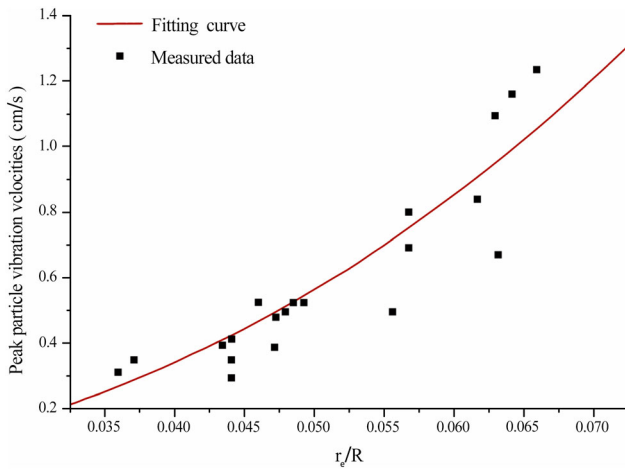


Fig. 10 Regression curve based on measured data

pattern of the test results showing a “large middle and two small ends” indicates consistency with the actual situation.

When the upper left part is blasted, the average error of the five measuring points is 14.78% and the minimum and maximum relative errors between the predicted values via the modified formula and measured values occurring at key points 1 and 3 are only 6.80% and 22.61%, respectively. Similarly, the average relative error of 10 measuring points is 14.61% and the minimum and maximum relative errors are 1.92% and 22.61%, respectively, when the upper right part of the tunnel is blasted. Therefore, the relatively small

errors between the predicted and measured values prove that the impact of blasting vibration on existing roads can be reflected by the proposed modified formula to some extent.

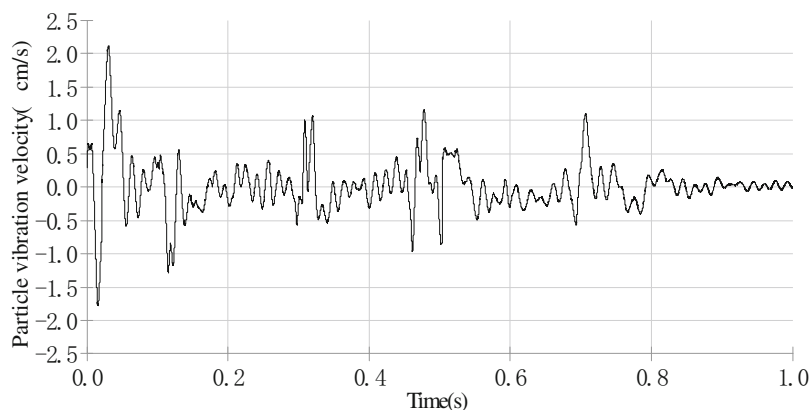
5 Conclusion

The blasting vibration during tunnel construction may damage the existing roads when newly constructed tunnels downtraverse these roads. The dynamic responses of existing roads subjected to blasting vibration must be evaluated thoroughly to guarantee the safety of existing roads during construction. Therefore, predicting PPV during construction blasting is very important. In this study, the modified formula of PPV is derived on the basis of the propagation and attenuation characteristics of explosion stress waves when the conditions of multihole and multi-stage blasting are considered. The modified formula of PPV is verified using field tests. The main conclusions of this study are presented as follows:

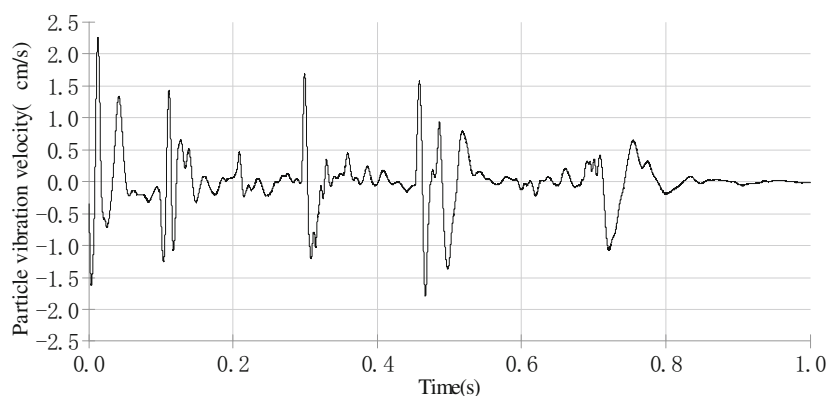
- (1) The attenuation formula of the propagation velocity of elastic stress waves in the elastomer is derived on the basis of stress wave theory. Moreover, the formula for predicting PPV is modified in the case of multihole and multistage blasting and then applied to Guanlinzi Tunnel, which downtraverses through National Highway 316. The results show that the

Table 6 Measured values and predicted values of PPVs for the key points of YK159 + 801 section

Blasting part	Measuring point number	Number of segments with maximum PPV	Maximum velocity direction	Measured one-way maximum PPV (cm/s)	Modified formula results		Sadov’s formula results	
					Maximum PPV (cm/s)	Relative error (%)	Maximum PPV (cm/s)	Relative error (%)
Upper left part	3	One segment	Z	1.99	1.54	22.61	5.92	197.50
	1	One segment	Z	2.35	2.19	6.80	8.04	242.24
	0	One segment	Z	1.46	1.81	23.90	6.92	374.23
	2	One segment	Z	1.19	1.33	11.70	5.19	336.42
	4	One segment	Z	0.56	0.61	8.92	2.64	371.95
Upper right part	3	One segment	Z	0.52	0.61	17.30	2.64	408.26
	1	One segment	Z	0.97	1.15	18.50	4.52	366.39
	0	One segment	Z	1.51	1.78	17.87	6.65	340.19
	2	One segment	Z	2.09	2.13	1.92	7.71	269.07
	4	One segment	Z	1.99	1.66	16.58	8.41	322.74



(a) Measured value of blasting vibration velocity of the key point 1 for the upper left part excavation



(b) Measured value of blasting vibration velocity of the key point 2 for the upper right part excavation

Fig. 11 Maximum vibration velocities of the key point of ZK159 + 801 section (Z direction)

modified formula can successfully reflect the propagation law of PPV under the condition of multihole and multistage blasting.

- (2) The damage or destruction of buildings (structures) subjected to blasting vibration is a process of energy transmission and transformation. The stress wave is affected by reflection or transmission and damping, and the energy is gradually attenuated in the process of medium propagation. According to the theoretical analysis and test results, the distribution law of PPVs shows that the section far from the blast source has a small vibration velocity in different sections, while the vibration velocity gradually decreases with increasing distance in the same section. The distribution pattern characterized by a “large middle and two small ends” shows consistency with the actual situation.

Acknowledgements This research was financially supported by the National Natural Science Foundation of China (Grant Nos. 51408054 sponsored), the Natural Science Foundation (2017JM5136, 2018JM5110) by the Science and Technology Department of Shaanxi

Province, the Housing and Urban–Rural Construction Foundation (2017-K55) by the Housing and Urban–Rural Department of Shaanxi Province, the Scientific Research Program (KLTLR-Y14-15) for Technology of Highway Construction and Maintenance Technology of National Transportation Industry Key Laboratory Technology Innovation, and the Scientific Research Program (2019217214GXRC008CG009-GXYD8.2) of the Science and Technology Department of Xi’an.

References

- Shin JH, Moon HG, Chae SE (2011) Effect of blast-induced vibration on existing tunnels in soft rocks. *Tunn Undergr Space Technol* 26(1):51–61. <https://doi.org/10.1016/j.tust.2010.05.004>
- Yu H, Yuan Y, Yu G, Liu X (2014) Evaluation of influence of vibrations generated by blasting construction on an existing tunnel in soft soils. *Tunn Undergr Space Technol* 43:59–66. <https://doi.org/10.1016/j.tust.2014.04.005>
- Simon L, Volker L, Jürgen H, Adrian R, Peter G (2014) Transient surface deformations caused by the gotthard base tunnel. *Int J Rock Mech Min Sci* 75:82–101. <https://doi.org/10.1016/j.ijrmms.2014.12.009>
- Yao Y, He C, Yan QX (2004) Numerical simulation of blasting control for small clear distance zone of dongjiashan tunnel (in Chinese). *Rock and Soil Mechanics* 25(S2):501–506. <https://doi.org/10.16285/j.rsm.2004.s2.107>

5. Ainalis D, Kaufmann O, Tshibangu J, Verlinden O, Kouroussis G (2017) Modelling the source of blasting for the numerical simulation of blast-induced ground vibrations: a review. *Rock Mech Rock Eng* 50(1):171–193. <https://doi.org/10.1007/s00603-016-1101-2>
6. Gui YL, Zhao ZY, Jayasinghe LB, Zhou HY, Goh ATC, Tao M (2018) Blast wave induced spatial variation of ground vibration considering field geological conditions (in Chinese). *Int J Rock Mech Mining Sci* 101:63–68. <https://doi.org/10.1016/j.ijrmms.2017.11.016>
7. Wang MN, Pan XM, Zhang CM, Wen XD, Wang KK (2004) Study of blasting vibration influence on close-spaced tunnel. *Rock Soil Mech* 25(3):412–414. <https://doi.org/10.1007/BF02911033>
8. Nateghi R (2011) Prediction of ground vibration level induced by blasting at different rock units. *Int J Rock Mech Min Sci* 48(6):899–908. <https://doi.org/10.1016/j.ijrmms.2011.04.014>
9. Standards of the People's Republic of China (GB6722–2014): Safety Regulations for Blasting, China Standard Press, Beijing, 2014
10. Sambuelli L (2009) Theoretical derivation of a peak particle velocity-distance law for the prediction of vibrations from blasting. *Rock Mech Rock Eng* 42(3):547–556. <https://doi.org/10.1007/s00603-008-0014-0>
11. Anders A (2004) In situ testing of young shotcrete subjected to vibrations from blasting. *Tunn Undergr Space Technol* 19:587–596. <https://doi.org/10.1016/j.tust.2004.01.059>
12. Hossein S, Seyed HK, Kourosh S, Mohammad ME, Mohammad E (2017) Optimization of a nonlinear model for predicting the ground vibration using the combinational particle swarm optimization-genetic algorithm. *J Afr Earth Sc* 133:36–45. <https://doi.org/10.1016/j.jafrearsci.2017.04.029>
13. Javier T, Rafael R (2006) FEM models including randomness and its application to the blasting vibration prediction. *Comput Geotech* 33:15–28. <https://doi.org/10.1016/j.compgeo.2006.01.003>
14. Shirani F, Jahed A, Abd M, Tahir MD, Murlidhar BR, Monjezi M, Wong HM (2016) Prediction of ground vibration due to quarry blasting based on gene expression programming: a new model for peak particle velocity prediction. *Int J Environ Sci Technol* 13(6):1453–1464. <https://doi.org/10.1007/s13762-016-0979-2>
15. Khandelwal M, Danial JA, Roohollah SF, Mohan Y, Muhd ZAM, Masoud M (2017) Classification and regression tree technique in estimating peak particle velocity caused by blasting. *Eng Computers* 33(1):45–53. <https://doi.org/10.1007/s00366-016-0455-0>
16. Wang GY, Liu JC (2012) Numerical analysis of effect of blasting vibration on adjacent roadway in 858 mines. *Appl Mech Mater* 238:783–786. <https://doi.org/10.4028/www.scientific.net/AMM.238.783>
17. Kahriman A, Ozer U, Aksoy M, Karadogan A, Tuncer G (2006) Environmental impacts of bench blasting at hisarcik boron open pit mine in Turkey. *Environ Geol* 50(7):1015–1023. <https://doi.org/10.1007/s00254-006-0274-5>
18. Luigi S (2009) Theoretical derivation of a peak particle velocity-distance law for the prediction of vibrations from blasting. *Rock Mech Rock Eng* 42(1):547–556. <https://doi.org/10.1007/s00603-008-0014-0>
19. Dehghani H, Ataee-pour M (2011) Development of a model to predict peak particle velocity in a blasting operation. *Int J Rock Mech Min Sci* 48(1):51–58. <https://doi.org/10.1016/j.ijrmms.2010.08.005>
20. Onederra I, Esen S (2004) An alternative approach to determine the Holmberg-Persson constants for modelling near field peak particle velocity attenuation. *Fragblast* 8(2):61–84. <https://doi.org/10.1080/13855140412331336151>
21. Lu WB, Hustrulid W (2002) An improvement to the equation for the attenuation of the peak particle velocity (in Chinese). *Eng Blast* 8(3):1–4. <https://doi.org/10.3969/j.issn.1006-7051.2002.03.001>
22. Wu L, Li F, Lu WB, Chen M, Xu F (2017) Vibration velocity threshold of a tunnel adjacent to surrounding layered rocks under blasting load (in Chinese). *Explos Shock Waves* 37(2):208–214. [https://doi.org/10.11883/1001-1455\(2017\)02-0208-07](https://doi.org/10.11883/1001-1455(2017)02-0208-07)
23. Rong Y, Zhao MJ, Huang HY (2005) Calculation and analysis of explosion loading of highway tunnels (in Chinese). *Technol Highway Transport* 1:91–94. <https://doi.org/10.3969/j.issn.1009-6477.2005.01.028>
24. Lu WB, Yang JH, Chen M (2011) Mechanism and equivalent numerical simulation of transient release of excavation load for deep tunnel (in Chinese). *Chin J Rock Mech Eng* 30(6):1089–1096. <https://doi.org/10.1631/jzus.B1000185>